

Copper Underpotential Deposition on Gold in the Presence of Polyethylene Glycol and Chloride

Yong-Da Chiu¹, Wei-Ping Dow^{1,*}, Yung-Fang Liu², Yuh-Lang Lee², Shueh-Lin Yau³, Su-Mei Huang⁴

¹ Department of Chemical Engineering, National Chung Hsing University, Taichung 40227, Taiwan

² Department of Chemical Engineering, National Cheng Kung University, Tainan 70101, Taiwan

³ Department of Chemistry, National Central University, Jhong-Li, Tao-Yuan 32001, Taiwan

⁴ Department of Chemical Engineering, Army Academy, Jhong-Li, Tao-Yuan 32092, Taiwan

*E-mail: dowwp@dragon.nchu.edu.tw

Received: 30 May 2011 / Accepted: 5 July 2011 / Published: 1 August 2011

Many articles have shown that polyethylene glycol (PEG), when combined with chloride ions, is a strong suppressor of copper overpotential deposition (OPD) on a copper substrate. However, few articles have explored the roles of PEG and chloride ions in copper underpotential deposition (UPD) when the cathodic substrate was polycrystalline gold. The individual roles and the interactions of PEG and chloride ions during Cu UPD on a polycrystalline gold electrode were characterized using cyclic voltammetry (CV). According to the CV patterns, a small amount of chloride ions strongly facilitated the Cu UPD at a more positive potential; PEG alone exhibited a similar CV pattern to that of the additive-free case. PEG significantly promoted the accelerating effect of chloride ions on Cu UPD, a result that is the opposite of what occurred during Cu OPD. A mechanism by which PEG-Cl accelerates Cu UPD was proposed. This mechanism also indirectly suggests that the suppressor of Cu OPD should be PEG-Cu⁺-Cl⁻, which could not form during Cu UPD on the polycrystalline gold electrode.

Keywords: Polyethylene glycol, suppressor, copper electrodeposition, underpotential deposition, overpotential deposition.

1. INTRODUCTION

Copper electrodeposition on a copper substrate has been comprehensively explored in industrial applications, particularly in the electronics industry [1-4]. The copper electrodeposition solutions formulated for the electronics industry have usually contained at least two or three organic additives, such as an accelerator, a suppressor and a leveler [5-9]. One commonly used suppressor is composed of polyethylene glycol (PEG) and chloride ions [10-17]. The inhibiting mechanism of PEG-

Cl in copper electrodeposition has been widely studied, and it has been shown that the PEG-Cu⁺-Cl⁻ complex adsorbed on the copper surface is the practical suppressor [10, 16, 17].

Because a common substrate adopted for copper plating was metallic copper, the copper plating process was performed within the range of overpotential deposition (OPD), meaning that the reductive potential of Cu²⁺ was more negative than the Nernst equilibrium potential of Cu²⁺/Cu [18]. Therefore, the proposed inhibiting mechanism of PEG-Cl was based on the copper OPD process. Recently, a new copper plating process, which uses a plating bath that contains no accelerator, was proposed [19, 20]. The required accelerator for copper electrodeposition was pre-adsorbed onto the seed layer of the sample in an independent pre-treatment bath. To enhance the yield, gold, rather than copper, was employed as the seed layer. This change was made because the disulfide group of the accelerator easily reacted with copper to destroy the seed layer, but a gold seed layer exhibited better chemical stability than did copper [19, 20]. The replacement of the seed layer material from copper to gold resulted in copper underpotential deposition (UPD) on the gold surface, meaning that the reductive potential of Cu²⁺ was more positive than the Nernst equilibrium potential of Cu²⁺/Cu [18].

Until now, most papers have focused on the effects of organic additives on copper OPD [5-17], but few papers have mentioned the effects of these additives, particularly PEG-Cl, on copper UPD [21, 22]. Kolb *et al.* [23] studied the effect of PEG-Cl on copper UPD and OPD on a Au(111) electrode. Inhibition of Cu OPD was observed when PEG and chloride ions were both present in solution, but PEG alone had a negligible impact, and chloride ions alone accelerated the deposition. In fact, many papers have studied the copper UPD process on a single-crystal gold electrode because it is easy to characterize [24-36]. However, the practical gold seed layer for the copper electroplating process is polycrystalline. Therefore, we have studied the effect of PEG-Cl on copper UPD using cyclic voltammetry (CV) to explore the role of PEG and chloride ions during copper UPD.

2. EXPERIMENTAL PART

CV was performed using a PGSTAT30 (Auto-Lab) potentiostat with a three-electrode setup. A polycrystalline gold electrode with a cross-sectional area of 0.0706 cm² (99.99%, Metrohm) was employed as the working electrode. The counter electrode was a platinum foil or a copper bar, depending on the presence of CuSO₄ in the electrolyte solution. A saturated mercurous sulfate electrode (SMSE) was employed as a reference electrode.

The mechanical pretreatment procedure included manually polishing the gold electrode to a mirror-finish with alumina slurry (particle sizes of 0.5 and 0.3 μm) and a polishing cloth. Finally, the electrode was rinsed with deionized (DI) water and cleaned ultrasonically in DI water for 5 min to remove residual alumina particles that could be trapped on the surface. After this mechanical pretreatment, the electrode surface was examined using an optical microscope (OM, Olympus BX51) to make sure there were no defects. The electrochemical pretreatment was performed by successive scans between gold redox potentials (from -0.7 V to 0.9 V *vs.* SMSE) in a 0.54 M H₂SO₄ aqueous solution at a scan rate of 50 mV s⁻¹. Usually, a stable gold redox pattern, which was the same as in previous work [37-39], was obtained after 6 cycles, demonstrating that a clean polycrystalline gold

surface had been obtained. The electrode was then rinsed with DI water and ultrasonicated in DI water for 5 min.

The redox CV patterns that occurred on the polycrystalline gold electrode in different electrolyte solutions were measured using a potentiostat with a three-electrode setup. The volume of the analytic solution was 100 mL, and the temperature of the solution was maintained at 25°C during analysis. The scan rate of the CV was 80 mV s⁻¹, starting at an open circuit potential (OCP) and was negative-going to the first return potential, positive-going to the second return potential and then returned to the OCP. The scan range depended on the presence of CuSO₄ in the electrolyte solution. The concentrations of chemicals used in the CV were 0.88 M CuSO₄, 0.54 M H₂SO₄, 200 ppm PEG with a molecular weight of 8000 mg mol⁻¹ (Fluka) and 10 to 60 ppm Cl⁻ (NaCl, Fisher, Certified ACS)

3. RESULTS AND DISCUSSION

3.1. CV of PEG and Cl⁻ in the absence of Cu²⁺

To understand the effect of chloride ions on the copper UPD, the electrolyte solutions that contained 0.54 M H₂SO₄ and different concentrations of chloride ions with no Cu²⁺ ions were first characterized by CV, as shown in Fig. 1.

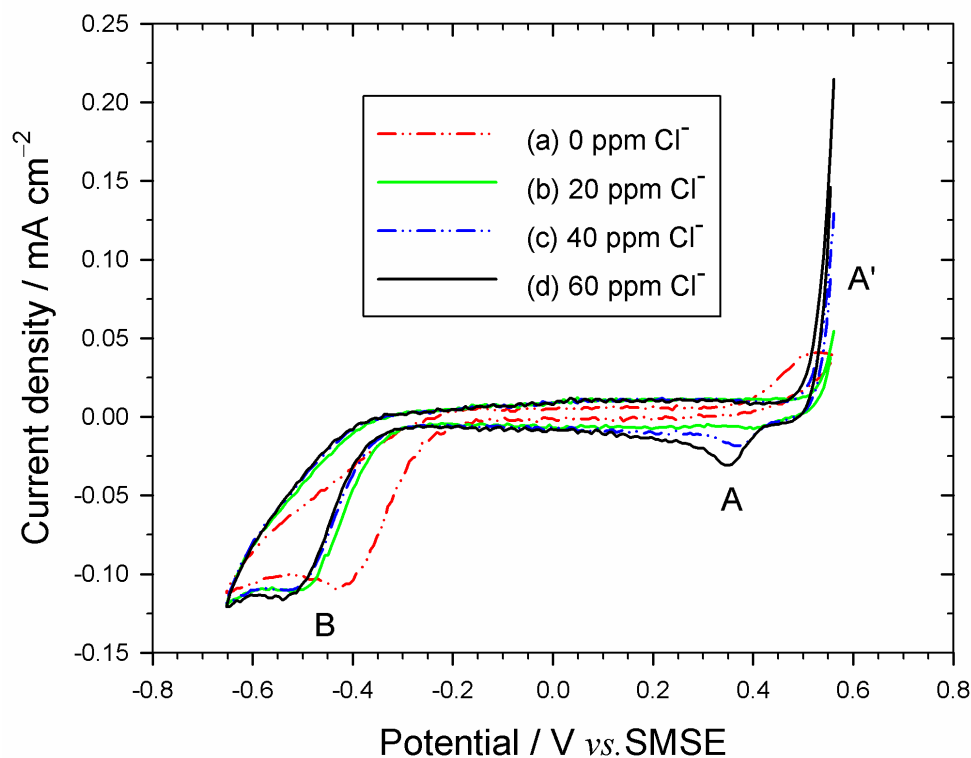


Figure 1. Cyclic voltammograms of polycrystalline gold electrodes in the presence of different chloride ion concentrations. The scan rate was fixed at 80 mV s⁻¹. The base solution was 0.54 M H₂SO₄.

Two current density peaks corresponding to reduction reactions, denoted by A and B, and one current density peak corresponding to an oxidation reaction, denoted by A', were observed in the CV. The magnitudes of peaks A' and A increased with the concentration of chloride ions. This redox is attributed to gold dissolution and reduction facilitated by chloride ions (i.e., $\text{Au} + 4\text{Cl}^- = \text{AuCl}_4^- + 3\text{e}^-$) [40, 41]. Therefore, these peaks did not appear in the absence of chloride ions, but a slight surface oxidation occurred (i.e., $2\text{Au} + 3\text{H}_2\text{O} = \text{Au}_2\text{O}_3 + 6\text{H}^+ + 6\text{e}^-$) [37-39], as recorded by curve (a). Peak B is attributed to the oxygen reduction reaction (ORR) in the acidic solution (i.e., $\text{O}_2 + 4\text{H}^+ + 4\text{e}^- = 2\text{H}_2\text{O}$) [42-43]. The addition of NaCl hampered the ORR because of the adsorptive effect of the cations and anions in the double layer, which caused a potential shift of the ORR.

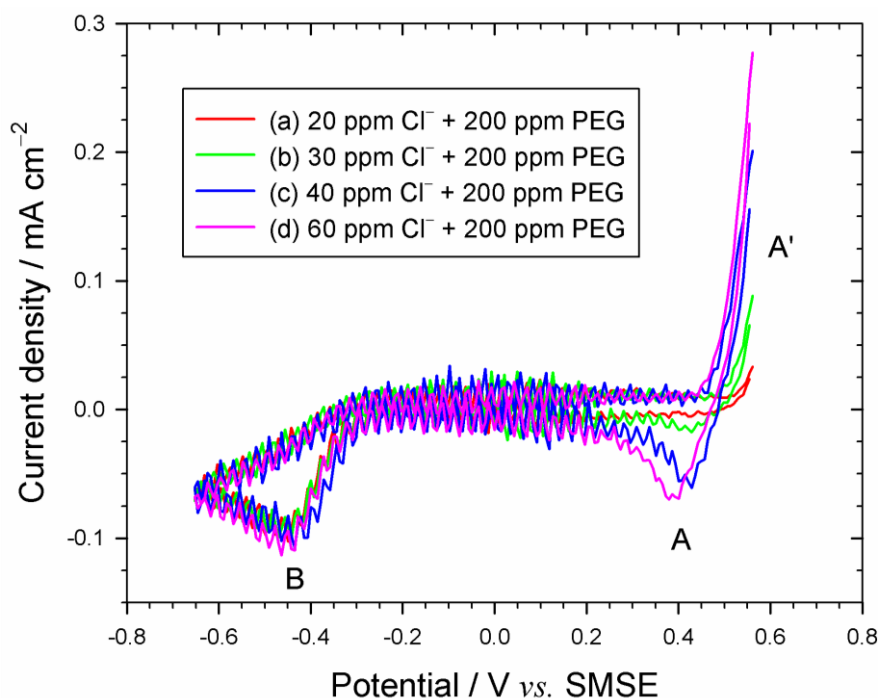


Figure 2. Cyclic voltammograms of polycrystalline gold electrodes in the presence of different chloride ion concentrations and 200 ppm PEG. The scan rate was fixed at 80 mV s^{-1} . The base solution was $0.54 \text{ M H}_2\text{SO}_4$.

When 200 ppm PEG was added to the electrolyte solutions that contained different concentrations of chloride ions, similar CV patterns to those in Fig. 1 were obtained, as shown in Fig. 2. However, strong oscillations in the current density were recorded in the CV. In addition, the magnitudes of peaks A' and A increased because of the addition of 200 ppm PEG, which indicates that PEG facilitated the gold redox in the presence of chloride ions. Similar results were also observed in the system using platinum as working electrode [44, 45]. They attributed the increase in oxidative current density after PEG addition to both platinum and PEG oxidation. The oscillation indicates that PEG, which is a polymer and a neutral wetting agent, could collide with the gold surface to fluctuate in the double layer on the gold electrode. Therefore, when PEG was present in the electrolyte solution, oscillation occurred, as shown in Fig. 3.

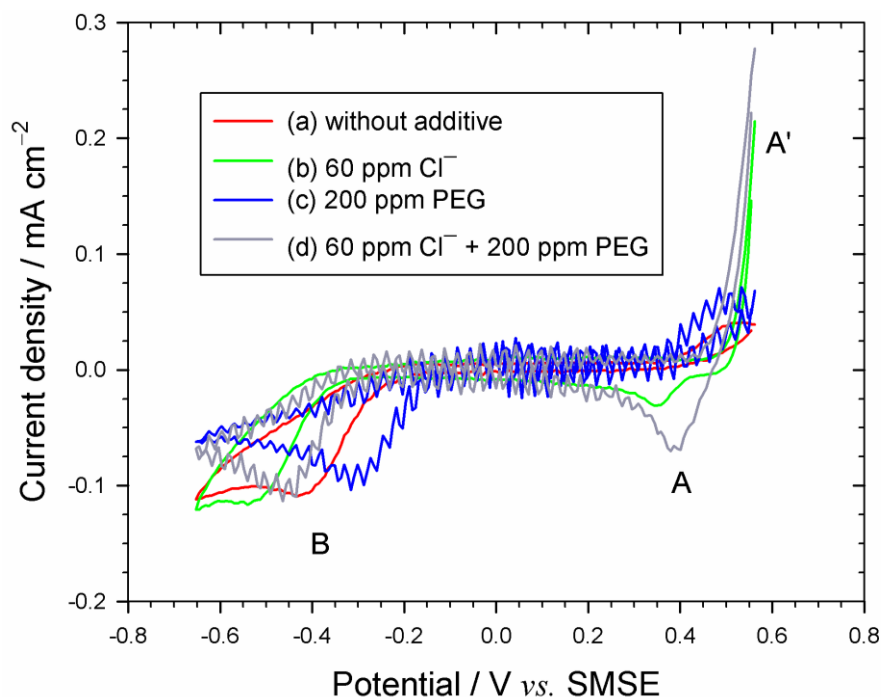


Figure 3. Cyclic voltammograms of polycrystalline gold electrodes in the absence and the presence of chloride ions and PEG. The scan rate was fixed at 80 mV s^{-1} . The base solution was $0.54 \text{ M H}_2\text{SO}_4$.

3.2. CV of Cl in the presence of Cu^{2+}

It is well known that chloride ions facilitate the reduction of Cu^{2+} to Cu^0 through a change in the electron transfer mechanism from an outer-sphere to an inner-sphere process [47]. In particular, chloride ions enhance the exchange current density of the rate-determining step in Cu^{2+} reduction (i.e., $\text{Cu}^{2+} + \text{e}^- = \text{Cu}^+$) [47]. The accelerating effect of chloride ions on Cu OPD also occurs during Cu UPD [28, 30-35]. To easily and clearly identify and characterize the Cu UPD in CV, the single-crystal Au(111) has been the most popular model electrode [24-31, 34, 35]. Two characteristic peaks of Cu UPD on Au(111) that are always observed in CV have been attributed to the copper deposition in the structure of $\sqrt{3} \times \sqrt{3} \text{R}30^\circ$ and 1×1 [24-27]. On Au(110) and Au(100) electrodes, only a 1×1 copper adlayer was observed by *in situ* scanning tunneling microscopy (STM) [26, 32, 33].

Cu UPD occurred on the polycrystalline Au electrode in a similar manner as on Au(111), as shown in Fig. 4. Two peaks that are typical of Cu UPD in the absence of chloride ions, namely C_1 and D, were observed and are shown in Fig. 4. The copper stripping peaks corresponding to C_1 and D are denoted by C_1' and D' . These Cu UPD and stripping patterns observed by CV were similar to those observed on the single-crystal gold electrodes with low and high indices [24-27, 36]. However, the profiles of these peaks were much broader than those that occurred on Au(111) because of the polycrystalline electrode used in this case [25]. The C_1/C_1' and D/D' peaks were assigned to the deposition and stripping of copper adatoms with $\sqrt{3} \times \sqrt{3} \text{R}30^\circ$ and 1×1 structures on Au(111) [24-27]. We did not assign the peaks to be $\sqrt{3} \times \sqrt{3} \text{R}30^\circ$ and 1×1 structures but rather to be Phase I and Phase II because of the polycrystalline gold electrode. When 10 ppm Cl^- ions were added to the electrolyte

solution, the D/D' peaks shrank, but the C₁/C₁' peaks became larger, which indicates that a trace amount of chloride ions promotes the copper atoms to be deposited preferentially on the Phase I structure rather than on the Phase II structure.

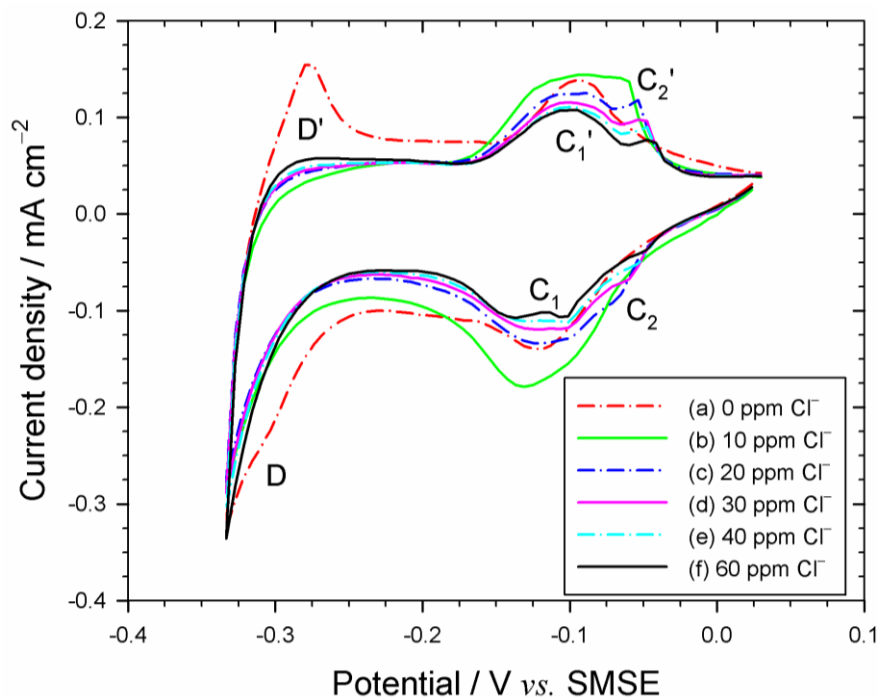


Figure 4. Cyclic voltammograms of polycrystalline gold electrodes in the presence of different chloride ion concentrations. The scan rate was fixed at 80 mV s^{-1} . The base solution was 0.88 M CuSO_4 and $0.54 \text{ M H}_2\text{SO}_4$.

This result was similar to the results obtained with the single-crystal gold electrodes and is attributed to the phase transformation of the copper adlayer from the $\sqrt{3} \times \sqrt{3} R30^\circ$ structure to a 5×5 structure on the Au(111) [28, 30, 31, 34, 35], from the 1×1 structure to a 2×1 structure on the Au(110) [32] and from the 1×1 structure to a $n \times 2$ structure on the Au(100) [33].

The magnitude of the D/D' peaks increased slightly with an increase in the chloride ion concentration. On the contrary, the magnitude of the C₁/C₁' peaks decreased with an increase in the chloride ion concentration, and two symmetric and sharp shoulders, namely C₂ and C₂', emerged, as shown in Fig. 4. It has been reported that the chloride ions could also adsorb on the gold electrodes in a specific phase, depending on the crystalline orientation and electrode potential [48, 49]. When chloride ions were present in the electrolyte solution, they induced copper atoms to be deposited in a different specific phase which differed from the phase obtained in the chloride-free electrolyte solution [28, 30-35]. The chloride-induced phase had an ordered adlayer superstructure, and its deposition and stripping were reversible; therefore, two symmetric and sharp spikes were formed at a more positive potential in the CV [28, 30-33]. The C₂/C₂' peaks are attributed to the formation/dissolution of the chloride-induced ordered adlayer. Their peak magnitudes decreased with an increase in the chloride ion

concentration because the chloride ions also adsorbed on the gold surface and occupied adsorbing sites [48, 49].

3.3. CV of PEG and Cl in the presence of Cu^{2+}

When both PEG and chloride ions were simultaneously present in the electrolyte solution, interesting results occurred, as shown in Fig. 5.

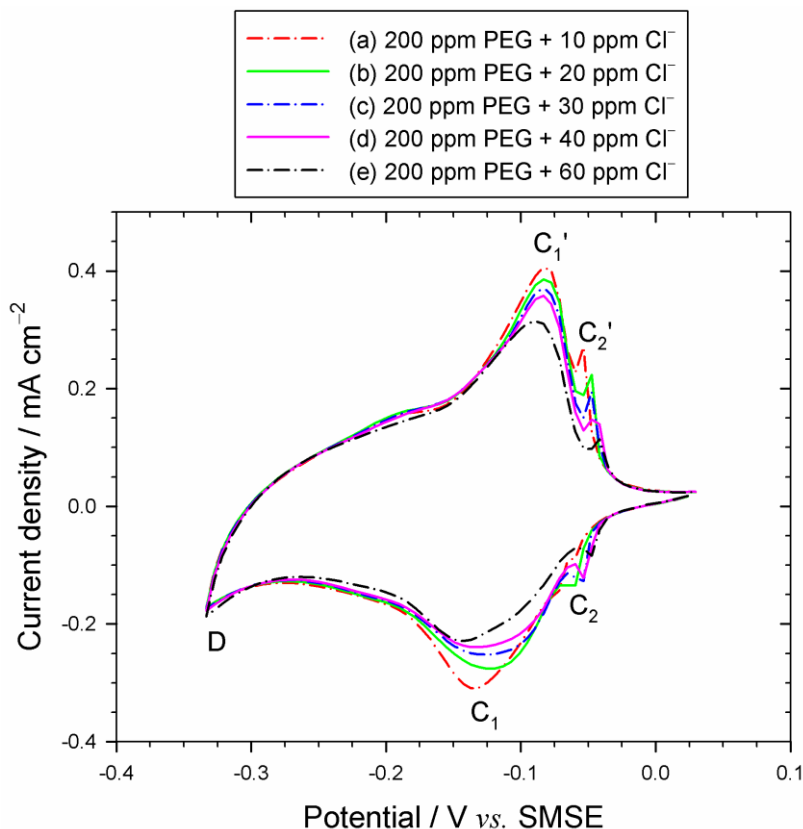


Figure 5. Cyclic voltammograms of polycrystalline gold electrodes in the presence of different chloride ion concentrations and 200 ppm PEG. The scan rate was fixed at 80 mV s^{-1} . The base solution was 0.88 M CuSO_4 and $0.54 \text{ M H}_2\text{SO}_4$.

The D/D' peaks shrank significantly, and ultimately, the peak D' disappeared. The C_1/C_1' and C_2/C_2' peaks became larger and sharper when both PEG and chloride ions were present. In addition, the magnitudes of the C_1/C_1' and C_2/C_2' peaks decreased with an increase in the chloride ion concentration. These results conflict with the previous understanding that PEG-Cl is a suppressor of Cu OPD [10-17]. Figure 5 shows that PEG-Cl is an accelerator for Cu UPD, suggesting that the inhibiting mechanism of PEG-Cl on Cu OPD does not apply to Cu UPD. Inversely, PEG-Cl facilitated Cu UPD at a more positive potential. The symmetric and sharp peaks, shown in Fig. 5, imply that more ordered copper adatoms were formed on the polycrystalline gold electrode because of the presence of PEG-Cl, and the copper deposition and stripping processes were reversible.

To characterize the accelerating effect of PEG-Cl on Cu UPD, several CV patterns are summarized in Fig. 6. The D/D' peaks only appeared in the absence of chloride ions, as illustrated by curves (a) and (c) in Fig. 6.

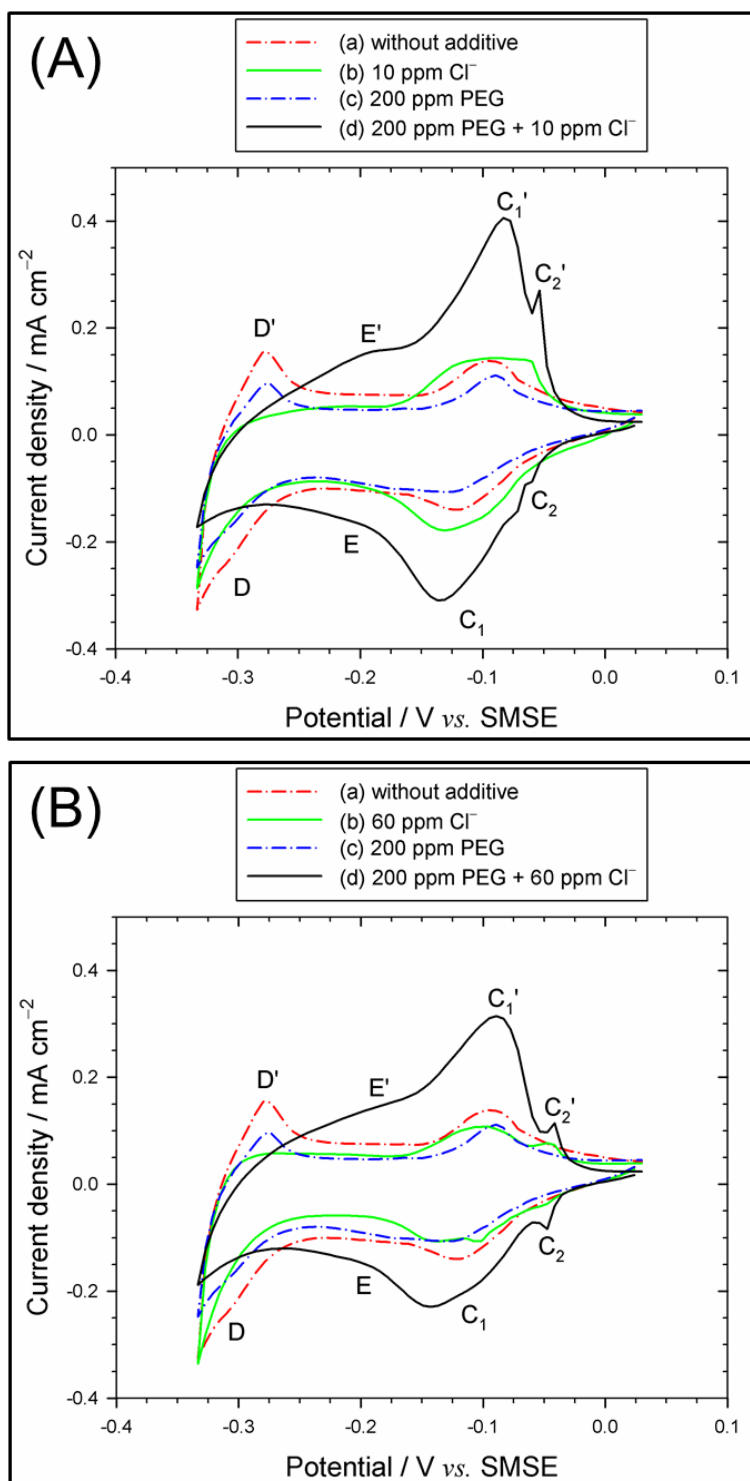
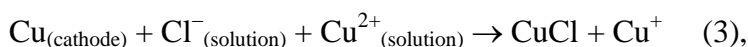
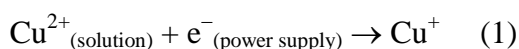


Figure 6. Cyclic voltammograms of polycrystalline gold electrodes in the absence and the presence of chloride ions and PEG. The scan rate was fixed at 80 mV s⁻¹. The base solution was 0.88 M CuSO₄ and 0.54 M H₂SO₄.

In the presence of chloride ions, the D/D' peaks shrank significantly, and the C₁/C₁' and C₂/C₂' peaks became larger, demonstrating that chloride ions facilitated the Cu UPD at a more positive potential. This facilitation of Cu UPD was further enhanced by adding PEG, as illustrated by curve (d) in Fig. 6, which resulted in the enhancement of the C₁/C₁' and C₂/C₂' peaks. In addition, the formation of the E/E' shoulder, shown in Fig. 6, could be attributed to the shift of the D/D' peaks towards a positive potential, which was caused by the synergy between the PEG and chloride ions. In other words, PEG-Cl strongly enhanced the coverage of Cu UPD on the polycrystalline gold but did not inhibit the Cu UPD.

According to the inhibiting mechanism of PEG-Cl on Cu OPD, the suppressor is composed of PEG-Cu⁺-Cl⁻ [10, 16, 17]. The source of Cu⁺ may have come one of the following reactions:



where reaction (1) is the electrochemical reduction of Cu²⁺ on the copper cathode, reaction (2) is the disproportionation reaction of the copper cathode with Cu²⁺ and reaction (3) is the surface corrosion of the copper cathode by chloride ions. These three reactions did not exist in the current system because the transition state of reaction (1) was skipped due to an inner-sphere electron transfer caused by the chloride ions [47], and the cathode required for reactions (2) and (3) was a gold material, rather than a copper material. Consequently, the suppressor, PEG-Cu⁺-Cl⁻, could not form during Cu UPD on the polycrystalline gold electrode. Instead, PEG-Cl accelerated Cu UPD, which indicates that PEG did not interact with chloride ions to form a blocking film on the polycrystalline gold electrode but functioned as a wetting agent that was capable of attracting Cu²⁺ ions. This attraction was caused by the ether groups of PEG. The attracted Cu²⁺ ions coming in contact with the chloride ions were instantly reduced to be the adatoms. The Cu²⁺ ions trapped by PEG-Cl differed from the hydrated Cu²⁺ ions, and their electrochemical redox was thermodynamically preferential. The redox peaks, shown in Fig. 6, were shifted toward a positive potential and enhanced relative to the case without PEG-Cl. In contrast with previous work [20], the so-called accelerator, bis(3-sulfopropyl)-disulfide (SPS), inhibited Cu UPD but accelerated Cu OPD [50-52]. The additives' roles were exchanged in Cu UPD and OPD.

4. CONCLUSIONS

The effect of PEG-Cl on Cu UPD on a polycrystalline gold electrode was characterized using CV. Chloride ions alone facilitated the Cu UPD at a more positive potential, and PEG alone did not significantly affect the Cu UPD. The interaction of PEG with Cl, which has been demonstrated to be a strong inhibiting agent for Cu OPD, did not inhibit Cu UPD but inversely facilitated more Cu²⁺ ions to

be deposited at a more positive potential, causing a significant shift and enhancement in the CV peaks. The acceleration of Cu UPD by the chloride ions caused by the addition of PEG was attributed to the wetting of PEG on the cathodic surface and the attraction of PEG to Cu^{2+} ions. The interaction of PEG with chloride ions changed the thermodynamic status of the trapped Cu^{2+} ions, which were easily and reversibly deposited and stripped at a more positive potential.

ACKNOWLEDGMENTS

This work was supported by the National Science Council of Taiwan under Contract No. NSC 96-2628-E-005-013-MY3.

References

1. P. C. Andricacos, C. Uzoh, J. O. Dukovic, J. Horkans, H. Deligianni, *IBM J. Res. Dev.* 12 (1998) 567.
2. D. Landolt, *J. Electrochem. Soc.* 149 (2002) S9.
3. M. Datta, *Electrochim. Acta* 48 (2003) 2975.
4. R. C. Alkire and R. D. Braatz, *AIChE J.* 50 (2004) 2000.
5. J. Reid, *Jpn. J. Appl. Phys. Part 1*, 40 (2001) 2650.
6. P. Taephaisitphongse, Y. Cao, A. C. West, *J. Electrochem. Soc.* 148 (2001) C492.
7. T. P. Moffat, D. Wheeler, D. Josell, *J. Electrochem. Soc.* 151 (2004) C262.
8. M. Hasegawa, Y. Negishi, T. Nakanishi, T. Osaka, *J. Electrochem. Soc.* 152 (2005) C221.
9. W.-P. Dow, C.-C. Li, Y.-C. Su, S.-P. Shen, C.-C. Huang, C. Lee, B. Hsu, S. Hsu, *Electrochim. Acta* 54 (2009) 5894.
10. M. Yokoi, S. Konishi, T. Hayashi, *Denki Kagaku oyobi Kogyo Butsuri Kagaku*, 52 (1984) 218.
11. J. D. Reid, A. P. David, *Plat. Surf. Finish.* 74 (1987) 66.
12. J. P. Healy, D. Pletcher, M. Goodenough, *J. Electroanal. Chem.* 338 (1992) 155.
13. D. Stoychev, C. Tsvetanov, *J. Appl. Electrochem.* 26 (1996) 1996.
14. J. J. Kelly, A. C. West, *J. Electrochem. Soc.* 145 (1998) 3472.
15. K. Doblhofer, S. Wasle, D. M. Soares, K. G. Weil, G. Ertl, *J. Electrochem. Soc.* 150 (2003) C657.
16. Z. V. Feng, X. Li, A. A. Gewirth, *J. Phys. Chem. B* 107 (2003) 9415.
17. M. E. Huerta Garrido and M. D. Pritzker, *J. Electrochem. Soc.* 156 (2009) D36.
18. W. J. Lorenz, G. Staikov, *Surf. Sci.* 335 (1995) 32.
19. W.-P. Dow, M.-Y. Yen, *Electrochem. Solid-State Lett.* 8 (2005) C161.
20. W.-P. Dow, Y.-D. Chiu, M.-Y. Yen, *J. Electrochem. Soc.* 156 (2009) D155.
21. E. D. Eliadis, R. C. Nuzzo, A. A. Gewirth, R. C. Alkire, *J. Electrochem. Soc.* 144 (1997) 96.
22. T. Y. Becky Leung, M. Kang, B. F. Corry, A. A. Gewirth, *J. Electrochem. Soc.* 147 (2000) 3326.
23. M. Petri, D. M. Kolb, U. Memmert, H. Meyer, *J. Electrochem. Soc.* 151 (2004) C793.
24. D. M. Kolb, *J. Vac. Sci. Technol. A* 4 (1986) 1294.
25. M. S. Zei, G. Qiao, G. Lehmpfuhl, D. M. Kolb, *Ber. Bunsenges. Phys. Chem.* 91 (1987) 349.
26. O. M. Magnussen, J. Hotlos, G. Beitel, D. M. Kolb, R. J. Behm, *J. Vac. Sci. Technol. B* 9 (1991) 969.
27. T. Hachiya, H. Honbo, K. Itaya, *J. Electroanal. Chem.* 315 (1991) 275.
28. N. Batina, T. Will, D. M. Kolb, *Faraday Discuss.* 94 (1992) 93.
29. I. H. Omar, H. J. Pauling, K. Jüttner, *J. Electrochem. Soc.* 140 (1993) 2187.
30. Z. Shi, S. Wu, J. Lipkowski, *J. Electroanal. Chem.* 384 (1995) 171.
31. Z. Shi, S. Wu, J. Lipkowski, *Electrochim. Acta* 40 (1995) 9.
32. F. Möller, O. M. Magnussen, R. J. Behm, *Electrochim. Acta* 40 (1995) 1259.

33. F. A. Möller, O. M. Magnussen, R. J. Behm, *Phys. Rev. B* 51 (1995) 2484.
34. J. Hotlos, O. M. Magnussen, R. J. Behm, *Surf. Sci.* 335 (1995) 129.
35. D. Krznarić, T. Gorićnik, *Langmuir* 17 (2001) 4347.
36. A. Kuzume, E. Herrero, J. M. Feliu, R. J. Nichols, D. J. Schiffrin, *J. Electroanal. Chem.* 570 (2004) 157.
37. L. Declan Burke, A. P. O'Mullane, *J. Solid State Electrochem.* 4 (2000) 285.
38. R. F. Carvalhal, R. S. Freire, L. T. Kubota, *Electroanalysis* 17 (2005) 1251.
39. J. Tkac, J. J. Davis, *J. Electroanal. Chem.* 621 (2008) 117.
40. Y.-C. Liu, L.-Y. Jang, *J. Phys. Chem. B* 106 (2002) 6748.
41. Y.-C. Liu, H.-H. Peng, *J. Phys. Chem. B* 108 (2004) 16654.
42. F. Gao, M. S. El-Deab, T. Okajima, T. Ohsaka, *J. Electrochem. Soc.* 152 (2005) A1226.
43. M. R. Miah, T. Ohsaka, *J. Electrochem. Soc.* 156 (2009) B429.
44. A. Méndez, P. Díaz-Arista, L. Salgado, Y. Meas, G. Trejo, *Int. J. Electrochem. Sci.* 3 (2008) 918.
45. A. Méndez, L. E. Moron, G. Orozco, R. Ortega-Borges, Y. Meas, G. Trejo, *Int. J. Electrochem. Sci.* 5 (2010) 1754.
46. V. S. Dilimon, N. S. Venkata Narayanan, S. Sampath, *Electrochim. Acta* 55 (2010) 5930.
47. Z. Nagy, J. P. Blaudeau, N. C. Hung, L. A. Curtiss, and D. J. Zurawski, *J. Electrochem. Soc.* 142 (1995) L87.
48. J. Lipkowski, Z. Shi, A. Chen, B. Pettinger, C. Bilger, *Electrochim. Acta* 43 (1998) 2875.
49. O. M. Magnussen, *Chem. Rev.* 102 (2002) 679.
50. P. M. Vereecken, R. A. Binstead, H. Deligianni, P. C. Andricacos, *IBM J. Res. Dev.* 49 (2005) 3.
51. Z. D. Schultz, Z. V. Feng, M. E. Biggin, A. A. Gewirth, *J. Electrochem. Soc.* 153 (2006) C97.
52. M. Tan, C. Guymon, D. R. Wheeler, J. N. Harb, *J. Electrochem. Soc.* 154 (2007) D78.